CONF-9606237--3





# CONTROL OF INTERFACE FRACTURE IN SILICON NITRIDE CERAMICS: INFLUENCE OF DIFFERENT RARE EARTH ELEMENTS

Ellen Y. Sun,[1] Paul F. Becher,[1] Shirley B. Waters,[1] Chun-Hway Hsueh,[1] Kevin P. Plucknett[1] and Michael J. Hoffmann[2]

[1]Metals and Ceramics Division, Oak Ridge National Laboratory, Oak Ridge, Tennessee 37831-6068
[2]University of Karlsruhe, Institute for Ceramics in Mechanical Engineering, Karlsruhe, Germany

## INTRODUCTION

The toughness of self-reinforced silicon nitride ceramics can be improved by enhancing crack deflection and crack bridging mechanisms.[1-3] Both mechanisms rely on the interfacial debonding process between the elongated β-$Si_3N_4$ grains and the intergranular amorphous phases. The various sintering additives used for densification may influence the interfacial debonding process by modifying (1) the thermal and mechanical properties of the intergranular glasses, which will result in different residual thermal expansion mismatch stresses;[4] and (2) the atomic bonding structure across the β-$Si_3N_4$/glass interface.[5] Earlier studies indicated that self-reinforced silicon nitrides sintered with different rare earth additives and/or different $Y_2O_3$:$Al_2O_3$ ratios could exhibit different fracture behavior that varied from intergranular to transgranular fracture.[6-8] However, no systematically studies have been conducted to investigate the influence of sintering additives on the interfacial fracture in silicon nitride ceramics. Because of the complexity of the material system and the extremely small scale, it is difficult to conduct quantitative analyses on the chemistry and stress states of the intergranular glass phases and to relate the results to the bulk properties.

In the current study, the influence of different sintering additives on the interfacial fracture behavior is assessed using model systems in which β-$Si_3N_4$ whiskers are embedded in SiAlRE (RE: rare-earth) oxynitride glasses. By systematically varying the glass composition, the role of various rare-earth additives on interfacial fracture has been examined. Specifically, four different additives were investigated: $Al_2O_3$, $Y_2O_3$, $La_2O_3$, and $Yb_2O_3$. In addition, applying the results from the model systems, the *R*-curve behavior of self-reinforced silicon nitride ceramics sintered with different $Y_2O_3$:$Al_2O_3$ ratios was characterized.

## DISCLAIMER

## EXPERIMENTAL PROCEDURE

In the model system, 5 vol.% β-$Si_3N_4$ whiskers were embedded in oxynitride-glasses. The processing parameters and the compositions of the glasses are listed in Table 1. The processing procedures are described in detail in Ref. 9. For each sample, glass formation, complete dissolution of the starting powders, and retention of β-$Si_3N_4$ whiskers were confirmed by x-ray diffraction analyses. The linear thermal expansion coefficients (α) and the glass transition temperatures ($T_g$) were measured using a dual rod dilatometer, following the procedures described in Ref. 10. Microstructural and compositional analyses were carried out using scanning electron microscopy (Hitachi S4100) equipped with energy dispersive spectrometry capable of light element detection.

**Table 1.** Compositions and processing conditions of the β-$Si_3N_{4(whisker)}$/oxynitride-glass model systems.

| Sample | Composition (eq.%) | | | | | Temp. | Time at Temp. |
|---|---|---|---|---|---|---|---|
| | Si | Al | Y or RE | O | N | (°C) | (minute) |
| AlY10 | 55 | 25 | 20 | 90 | 10 | 1700 | 1 |
| AlY20-I | 55 | 25 | 20 | 80 | 20 | 1700 | 6 |
| YAl10 | 55 | 10 | 35 | 90 | 10 | 1650 | 1 |
| YAl20-I | 55 | 10 | 35 | 80 | 20 | 1700 | 8 |
| AlY20-II | 55 | 25 | 20 | 80 | 20 | 1600* | 60* |
| YAl20-II | 55 | 10 | 35 | 80 | 20 | 1600* | 60* |
| LaAl | 50 | 25 | 25 | 67 | 33 | 1680 | 30 |
| YbAl | 50 | 25 | 25 | 67 | 33 | 1680 | 30 |
| La | 57 | 0 | 43 | 79 | 21 | 1700 | 4 |

* AlY20-II and YAl20-II were obtained by annealing AlY20-I and YAl20-I under these conditions.

The debonding response of the whisker/glass interface in the different systems was evaluated by an indentation-induced crack-deflection method, as illustrated by the schematical diagram in Figure 1(a). A cube-corner diamond indenter with a 30-35 gram applied load was used to generate cracks in the glass. When the indentation crack plane intersects the longitudinal axis of the whisker, the crack will either deflect at the whisker/glass interface or penetrate the whisker, depending on the angle of incidence (θ). For a specific interface, it becomes increasingly more difficult for a crack that is propagating in the matrix to deflect at and travel along the interface as θ is increased towards 90°. By characterizing the interface debond length, $l_{db}$, versus θ, the maximum angle of incidence for the onset of interfacial debonding ($\theta_{crit}$) can be determined, as shown in Figure 1(b). By comparing the $\theta_{crit}$ and $l_{db}$ values, the interfacial debonding energy in different systems can be assessed.

Self-reinforced silicon nitride ceramics sintered with different $Y_2O_3$:$Al_2O_3$ additive ratios (but same total amounts) were studied in conjunction with the $Si_3N_{4(whisker)}$/oxynitride-glass model systems. Three different $Y_2O_3$:$Al_2O_3$ ratios were employed: 1:1, 2:3 and 3:1

(ratio in eq.%). The fraction of large elongated grains in these samples was controlled by incorporating 2 wt.% elongated β-$Si_3N_4$ seeds into the ceramics, following the procedures described in Ref. 11. The *R*-curve behavior of the ceramics was characterized *in-situ* using an applied moment DCB testing stage operated either under an optical microscope (Nikon MM-11) or in the chamber of an SEM (Hitachi S4100).[12]

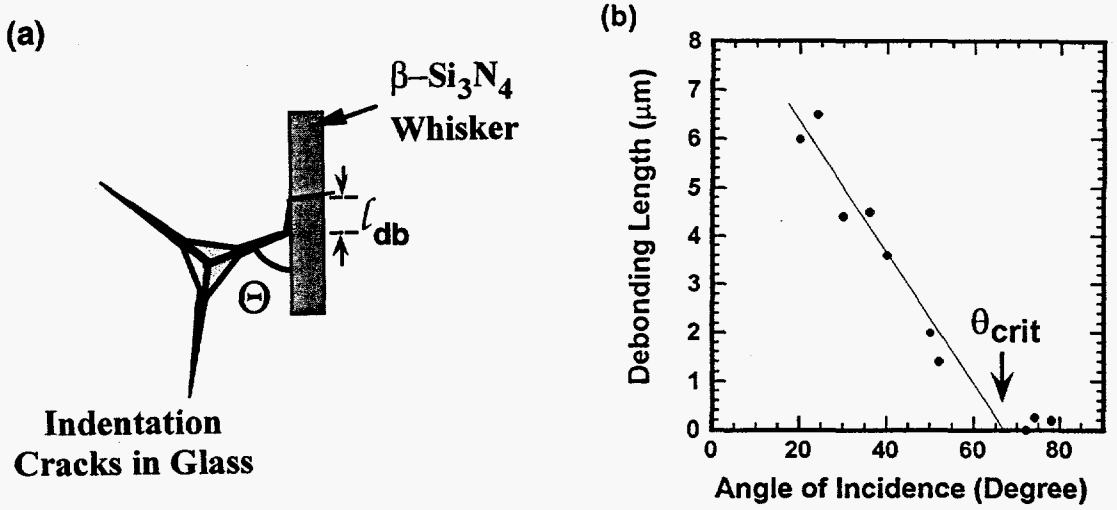


**Figure 1.** (a) Schematic diagram of the debonding experiment; and (b) data analyses of the debonding experiment. $\theta_{crit}$ can be determined by plotting $l_{db}$ versus θ.

## RESULTS AND DISCUSSION

### Interfacial Debonding Behavior in the $Si_3N_{4(whisker)}$/Oxynitride-Glass Systems

The interfacial debonding behavior in the $Si_3N_4$/Si-Al-Y glass systems processed at high temperatures for a short period of time (AlY10, AlY20-I, YAl10 and YAl20-I)[9] is briefly summarized here. As shown in Figure 2, systems AlY10, YAl10 and YAl20-I showed similar debonding behaviors, while system AlY20-I exhibited much lower $\theta_{crit}$ and $l_{db}$ values compared to the other three systems, indicating a higher interfacial debonding energy. Microstructural characterization revealed formation of a β′-SiAlON layer at the $Si_3N_4$/glass interface in system AlY20-I, which was absent in the other systems.[5] These results indicate that the $\theta_{crit}$ and $l_{db}$ values are decreased when an interfacial SiAlON layer forms.

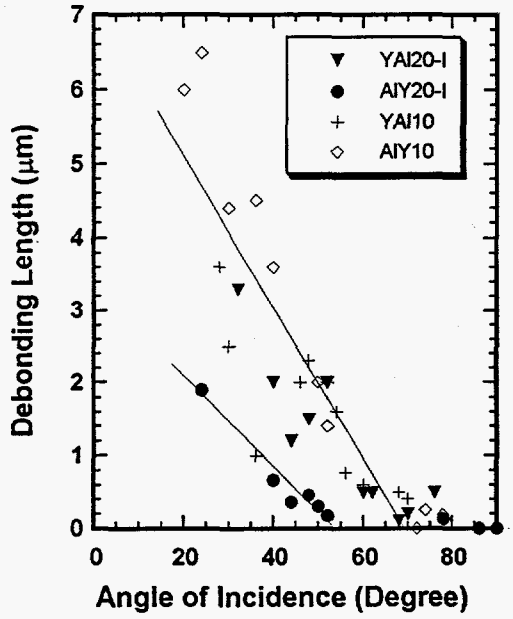


**Figure 2.** Debonding behavior in the AlY and YAl systems.

Phase equilibrium indicates that the formation of β′-SiAlON phase from the Si–Al–Y oxynitride glasses is thermodynamically favorable when the nitrogen content is greater than 16 eq.%.[13] However, the kinetics of the interfacial phase formation depends upon the specific glass composition and processing conditions. Among the four systems discussed above, SiAlON-formation was observed only in system AlY20-I under the processing conditions employed (1600°–1700°C for several minutes). It is possible for SiAlON-formation to occur in the other high-nitrogen system (YAl20) with extended holding times at elevated temperatures.

The formation of SiAlON layers and its influence on the interfacial debonding strength were studied by examining the microstructure evolution and interfacial debonding behavior of systems AlY20-II and YAl20-II, which were obtained by annealing AlY20-I and YAl20-I respectively. β′-SiAlON growth on the β-$Si_3N_4$ whisker indeed occurred in the YAl20 system, as shown in Figure 3(a). Furthermore, the interfacial debonding behavior of system YAl20 changed dramatically after the annealing treatment (Figure 3(b)). On the other hand, the debonding behaviors of system AlY20 remained the same after the annealing treatment. Compared with the data in Figure 2, it is noted that the $\theta_{crit}$ values are significantly lower in all the systems with SiAlON-formation (AlY20-I&II and YAl20-II) — ~50° in systems with SiAlON versus ~70° without SiAlON. These results appear to confirm that SiAlON growth on the β-$Si_3N_4$ grains induces in a high interfacial debonding energy.

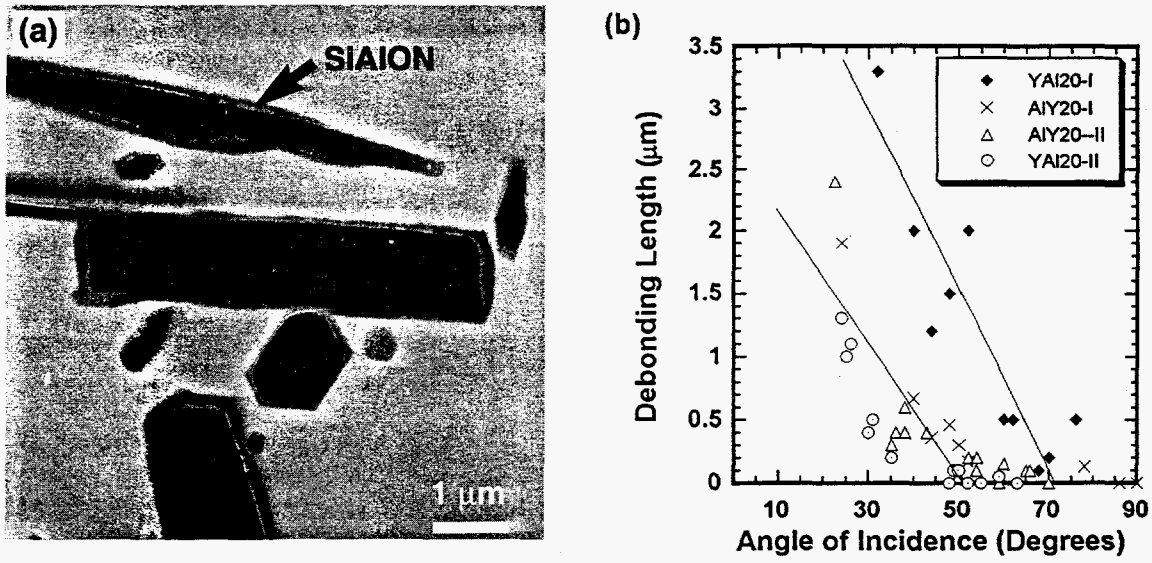


**Figure 3.** (a) A SiAlON layer formed on surface of the β-$Si_3N_4$ whiskers in system YAl20 after the annealing treatment; and (b) debonding behavior in systems AlY20 and YAl20 before and after the annealing treatments.

The SiAlON formation has a similar influence on the interfacial debonding energy in other Si-Al-RE-O-N (RE: rare earth) glass systems. SiAlON growth occurred in the LaAl and YbAl systems because the materials were prepared at high temperatures for 30 minutes. The SiAlON growth band exhibited a similar structure as that shown in Figure 3(a). Comparing with the AlY and YAl systems, the $\theta_{crit}$ and $l_{db}$ values in the LaAl and YbAl systems are comparable to those of the AlY and YAl series with SiAlON formation, as illustrated in Figure 4.

Systems not containing Al were also studied, where the SiAlON formation would not be an influence on the interfacial debonding behavior. Specifically, systems with Si-La-O-N glasses were examined. The $\theta_{crit}$ and $l_{db}$ values in the La-system were compared with those in the AlY and YAl systems without SiAlON formation, as shown in Figure 5. Compared with the LaAl system with SiAlON formation, interfacial debonding was enhanced in the Al-free La system.

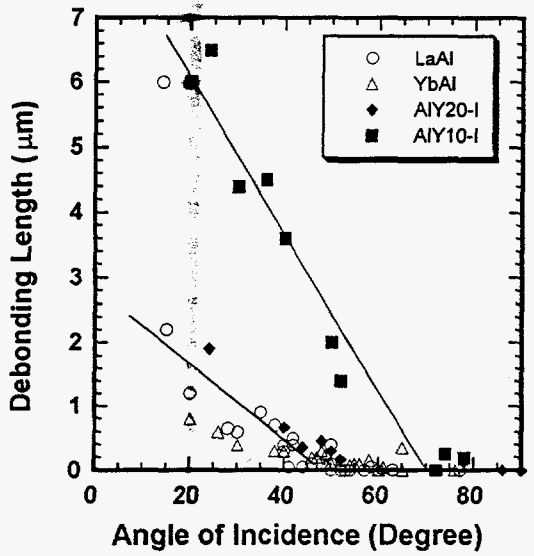


**Figure 4.** Debonding behavior in the LaAl and YbAl systems.

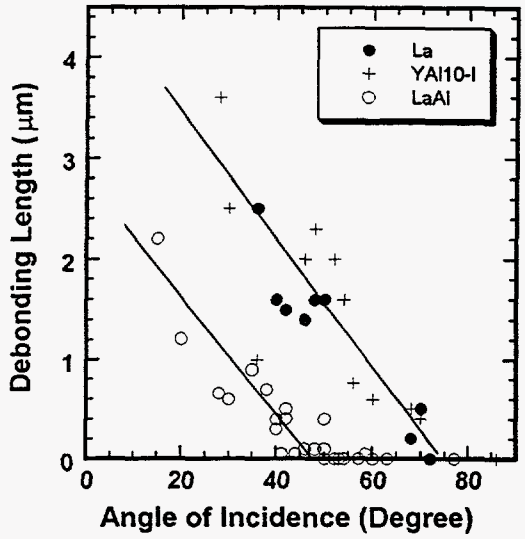


**Figure 5.** Debonding behavior in the La based systems.

## Residual Thermal Mismatch Stresses

The residual thermal mismatch stresses in these $Si_3N_{4(whisker)}$/oxynitride-glass systems were analyzed using a modified Eshelby model, in which the whiskers were simulated as ellipsoidal inclusions with an aspect ratio of 10:1.[14, 15] The thermal and mechanical properties of the glasses and the β-$Si_3N_4$ crystal used in the predictions were measured (Table 2). Previous studies found that the elastic modulus of oxynitride glasses does not vary significantly with composition[9] and the residual thermal mismatch stresses were more sensitive to the thermal properties than the mechanical properties. Therefore, an average elastic modulus value of 145 GPa was used in the current calculations. Poisson ratios of the whiskers and glasses were assumed to be 0.29 and 0.26 respectively.

**Table 2.** Measured thermal and mechanical properties of the oxynitride glasses and the β-$Si_3N_4$ crystal.

| Sample | AlY10 | AlY20 | YAl10 | YAl20 | LaAl | YbAl | La | β-$Si_3N_4$ | |
|---|---|---|---|---|---|---|---|---|---|
| α ($10^{-6}$/°C) | 5.25 | 5.17 | 6.66 | 6.38 | 6.5 | 5.9 | 7.2 | 2.01[a] | 2.84[b] |
| $T_g$ (°C) | 915 | 950 | 970 | 1005 | 1030 | 990 | 1010 | --- | |
| E (GPa) | 145 | | | | | | | 380 | |

[a]a-axis, [b]c-axis, Ref. 16

Stress analyses revealed that the resultant radial and axial thermal expansion mismatch stresses within a rod embedded in oxynitride glass were compressive due to the lower thermal expansion coefficient of the silicon nitride. The relationship between the compressive radial residual stresses and the $\theta_{crit}$ and $l_{db}$ values are shown in Figures 6(a) and 6(b). (The axial residual stresses show a similar trend. The stress levels only change ~2% and the ranking of the stresses remains the same when the SiAlON layer is considered.[9]) The results indicate that SiAlON formation determines the $\theta_{crit}$ values while the influence of the residual thermal mismatch stresses appears to be negligible (Figure 6(a)). On the other hand, it is noticed that among systems without the SiAlON formation, the debonding length at a fixed angle of incidence generally increases with decreasing residual stresses (Figure 6(b)). However, no such relationship was observed in systems with the SiAlON formation.

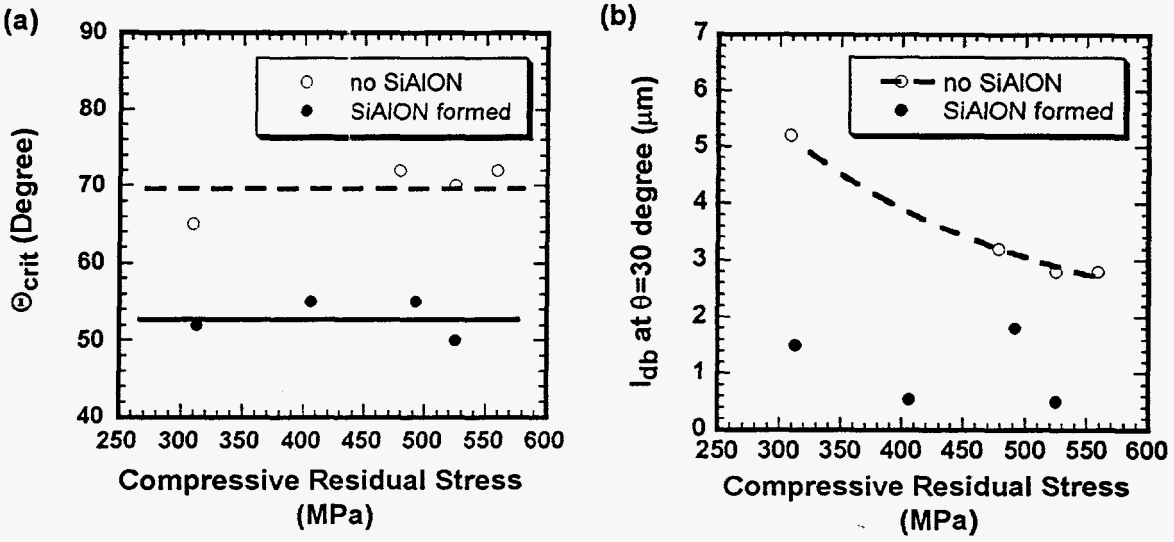


**Figure 6.** Relationship between the compressive radial residual stresses and the (a) $\theta_{crit}$ and (b) $l_{db}$ values.

## *R*-Curve Behavior of Seeded Silicon Nitrides with Different Sintering Additives

The seeded silicon nitride ceramics exhibited *R*-curve responses that were dependent on the ratio of yttria to alumina sintering additives. As shown in Figure 7, the materials sintered with the highest $Y_2O_3$:$Al_2O_3$ ratio exhibit the highest steady-state toughness and a steeply rising *R*-curve, while the materials sintered with the lowest $Y_2O_3$:$Al_2O_3$ ratio have the lowest steady-state toughness. *In-situ* observation of crack propagation and interaction with microstructural features indicated that crack-deflection and bridging occurred more readily in the higher yttria-content samples (Figure 8). However, the main cause for the different interface fracture behavior in these three ceramics was residual stresses, instead of interfacial phase formation as shown in the whisker/glass model systems, because SiAlON growth was present in all the three ceramics studied due to the long processing time at elevated temperatures. Also, it is possible that the influence of residual stresses on the interface fracture is greater in the ceramics than in the whisker/glass systems due to the significantly different volume fractions of the glassy phases. Ongoing research is focusing on the measurement and analytical modeling of residual stresses in silicon nitride ceramics.

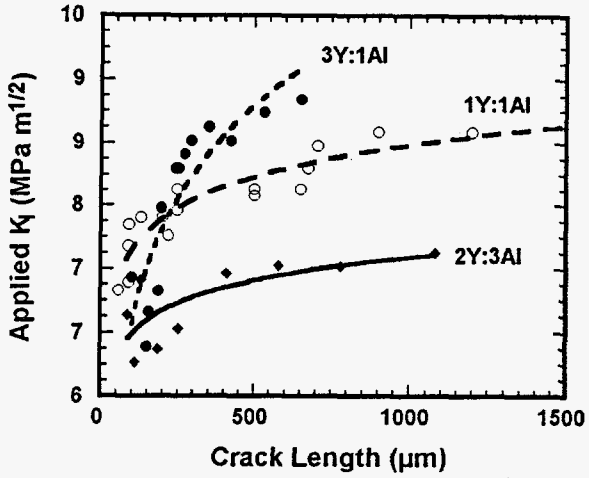


**Figure 7.** *R*-curve response of self-reinforced silicon nitrides sintered with different yttria to alumina additives.

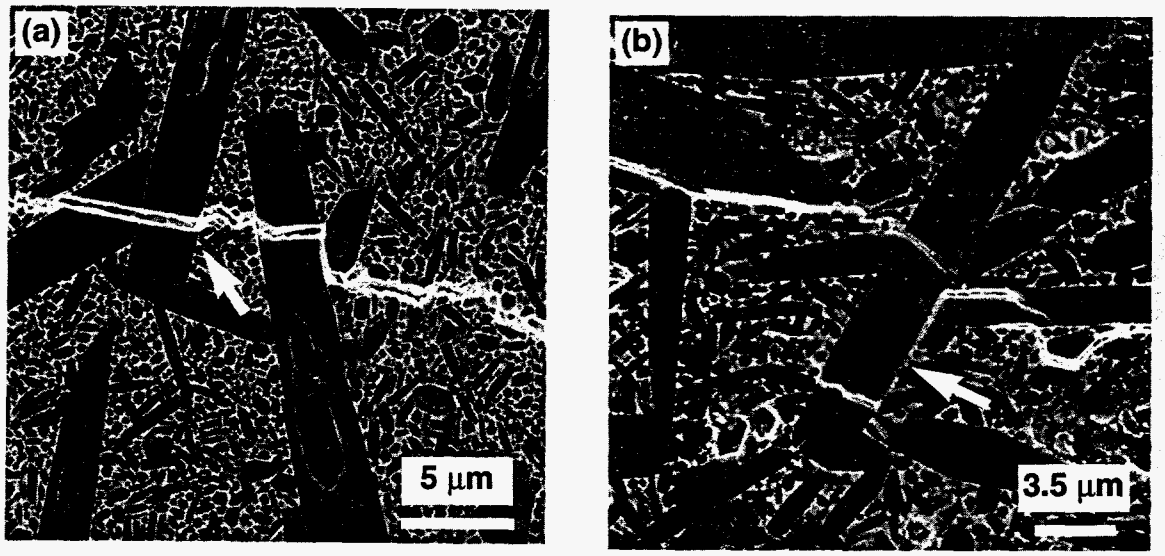


**Figure 8.** Crack deflection and bridging by the elongated grains in seeded silicon nitride sintered with different $Y_2O_3$:$Al_2O_3$ additive ratios, (a) 2Y:3Al and (b) 3Y:1Al.

## CONCLUSION

In $Si_3N_{4(whisker)}$/oxynitride-glass model systems, interfacial debonding behavior is determined by the interfacial microstructure and chemistry. In Si-Al-RE(Y)-O-N glasses, the interfacial debonding energy increases significantly with SiAlON formation. Al-free glasses enhance interfacial debonding by inhibiting SiAlON formation. Compared to the interfacial microstructure/chemistry, the residual thermal mismatch stresses are a secondary influence on the debonding behavior. In systems without SiAlON formation, the residual stresses modify the debonding length. In self-reinforced silicon nitride ceramics, a higher yttria to alumina additive ratios resulted in a higher steady state toughness. Sophisticated experimental and analytical-modeling work are required to understand the influence of the residual stresses on the interfacial fracture behavior in self-reinforced silicon nitride ceramics.

## ACKNOWLEDGMENTS

The authors thank Drs. K. Hirao and M. Brito of the National Industrial Research Institute-Nagoya for their assistance and the MITI Agency for International Science and Technology Fellowship (Japan) for supporting KPP producing the silicon nitride ceramics at NIRI-Nagoya. Drs. H. T. Lin and E. Lara-Curzio are thanked for reviewing the manuscript. Research is sponsored by the U.S. Department of Energy, Division of Materials Sciences, Office of Basic Energy Sciences, under contract DE-AC05-96OR22464 with Lockheed Martin Energy Research Corp. and by appointments of EYS and KPP to the Oak Ridge National Laboratory Postdoctoral Research Associates Program, which is administered jointly by the Oak Ridge Institute for Science and Education and Oak Ridge National Laboratory.

## REFERENCES

1. P. F. Becher, S. L. Hwang, and Chun-Hway Hsueh, Using microstructure to attack the brittle nature of silicon nitride ceramics, *MRS Bull.* 20[2]:21 (1995).
2. T. Kawashima, H. Okamoto, H. Yamamoto, and A. Kitamura, Grain size dependence of the fracture toughness of silicon nitride ceramics, *J. Am. Ceram. Soc. Japan,* 99:1 (1991).
3. P. Sajgalik, J. Dusza, and M. J. Hoffmann, Relationship between microstructure, toughening mechanism, and fracture toughness of reinforced silicon nitride ceramics, *J. Am. Ceram. Soc.,* 78[10]:2619 (1995).
4. I. M. Peterson and T. Y. Tien, Effect of grain boundary thermal expansion coefficient on the fracture toughness in silicon nitride, *J. Am. Ceram. Soc.,* 78[9]:2345 (1995).
5. E. Y. Sun, K. B. Alexander, P. F. Becher, S. L. Hwang, $\beta$-$Si_3N_4$ whiskers embedded in oxynitride-glasses: interfacial microstructure, *J. Am. Ceram. Soc.,* in print.
6. Y. Tajima, K. Urashima, M. Watanabe, and Y. Matsuo, Fracture toughness and microstructure evaluation of silicon nitride ceramics, in *Ceramic Transactions, Vol. 1,* E. R. Fuller and H. Hausner, ed., Am. Ceram. Soc., Westerville (1988).
7. Y. Tajima, Development of high performance silicon nitride ceramics and their application, in *MRS Proc., Vol. 287,* I. W. Chen, P. F. Becher, M. Mitomo, G. Petzow and T. S. Yen, ed., MRS, Pittsburgh (1993).
8. G. Wotting and G. Ziegler, Influence of powder properties and processing conditions on microstructure and mechanical properties of sintered $Si_3N_4$, *Ceramics Intl.,* 10[1]:18 (1984).
9. P. F. Becher, E. Y. Sun, C. H. Hsueh, K. B. Alexander, S. L. Hwang, S. B. Waters, and C. G. Westmoreland, Debonding of interfaces between beta-silicon nitride whiskers and Si-Al-Y oxynitride glasses, *Acta Metall.,* in print.
10. E. Y. Sun, P. F. Becher, S. L. Hwang, S. B. Waters, G. M. Pharr, and T. Y. Tsui, Properties of silicon-aluminum-yttrium oxynitride glasses, *J. Non-Crystal. Solids,* in print.
11. K. Hirao, M. Ohashi, M. E. Brito, and S. Kanzaki, Processing strategy for producing highly anisotropic silicon nitride, *J. Am. Ceram. Soc.,* 78[6]:1687 (1995).
12. P. F. Becher, C. H. Hsueh, K. B. Alexander, and E. Y. Sun, Influence of reinforcement content and diameter on the *R*-curve response in SiC-whisker-reinforced alumina, *J. Am. Ceram. Soc.,* 79[2]:298 (1995).
13. A. Drew, *Nitrogen Glass,* P. Evans, ed., the Pathenon Press, Casterton Hall, U.K. (1986).
14. C. H. Hsueh and P. F. Becher, Residual thermal stresses in ceramic composites, part I with ellipsoidal inclusions, *Mater. Sci. Eng.* A212:22 (1996).
15. C. H. Hsueh and P. F. Becher, Residual thermal stresses in ceramic composites, part II with short fibers inclusions, *Mater. Sci. Eng.* A212:29 (1996).
16. C. M. B. Henderson and D. Taylor, Thermal expansion of the nitrides and oxynitride of silicon in relation to their Structure, *Trans. Brit. Ceram. Soc.* 74[2]:49 (1975).